Supplementary Information (SI) for ChemComm.
This journal is © The Royal Society of Chemistry 2026

Electronic Supporting Information for:

The Silver Sputnik. Evaluation of the Exohedral Dynamic in $[C_{60}M]^+$ (M = Cu, Ag, Au)

Alvaro Muñoz-Castro[a*]

[a]*Facultad de Ingeniería, Universidad San Sebastián, Bellavista 7, Santiago, 8420524, Chile.*

E-mail: alvaro.munozc@uss.cl

Content.

Computational details. Page S2

Table S1. C_{60}-M distance (dC_{60}-M, Å), charge distribution (q^{C60} and q^{M}, |e|), and the Energy Decomposition Analysis (EDA) for the C_{60}-M interaction for the studied series (kcal/mol). Page S4

Figure S1. Molecular dynamics simulations (200 ps) revealing the distinct dynamic domains over the C_{60} fullerene surface at 400.15 K, denoting the overlap of all the metal trajectories. Page S5

Figure S2. NICS contour plots for the studied species. Page S6

Computational Details

Calculations were done using the ADF2024 code,[1] involving Triple-ξ and two polarization functions (STO-TZ2P) basis sets within the hybrid PBE0 functional.[2] The pairwise Grimme correction (D3)[3–6] and Becke-Johnson damping functions[7,8] were taken into account for the empirical dispersion correction to DFT (DFT-D3BJ). The molecular structures were optimized through the analytical energy gradient method implemented by Versluis and Ziegler[9] at the TZ2P/PBE0-D3BJ level without any symmetry restraints. Charge distribution analysis was obtained from the Natural Population Analysis (NPA).

Molecular dynamics (MD) calculations were performed by using the semiempirical tight-binding Hamiltonian GFN2-xTB, as implemented in the xTB program suite.[10,11] The previous optimized geometries of the host-guest pairs were used as the initial structures for all xTB-based MD simulations. Trajectories were propagated in the canonical NVT ensemble at 328.15 K using the built-in MD integrator of xTB. The MD simulations were conducted over 500 ps with an integration time step of 2.0 fs, saving configurations every 50 fs. The SCC convergence threshold during dynamics was set to the default value, and velocities were not reused from previous runs.

The calculated nuclear chemical shieldings (σ) were referenced to that of C_{60} to obtain the calculated ^{13}C-NMR chemical shifts (δ) using the following formula:

$$\delta_i = \sigma(C_{60}) - \sigma_i + \delta(C_{60})$$

where $\delta(C_{60})$ is taken as 143.15 ppm,[12] $\sigma(C_{60})$ is the calculated chemical shielding of C_{60} (53.10 ppm), and (i) is the carbon atom under consideration. Calculations done within the GIAO formalism at the ADF2024 suite,[1] involving an all-electron triple-ζ Slater basis set plus the double-polarization functions within the hybrid PBE0 functional.[2,13] Evaluation of the resulting magnetic behavior is obtained at the same level of theory by a two-dimensional array of nucleus-independent shielding tensors (NICS).[14–16]

References

[1] Amsterdam Density Functional (ADF 2024) Code, Vrije Universiteit: Amsterdam, The Netherlands. Available at: http://www.scm.com.

[2] C. Adamo, V. Barone, Toward reliable density functional methods without adjustable parameters: The PBE0 model, J. Chem. Phys. 110 (1999) 6158–6170. https://doi.org/10.1063/1.478522.

[3] S. Grimme, Accurate description of van der Waals complexes by density

functional theory including empirical corrections, J. Comput. Chem. 25 (2004) 1463–1473. https://doi.org/10.1002/jcc.20078.

[4] S. Grimme, Semiempirical GGA-type density functional constructed with a long-range dispersion correction, J. Comput. Chem. 27 (2006) 1787–1799. https://doi.org/10.1002/jcc.20495.

[5] S. Grimme, J. Antony, S. Ehrlich, H. Krieg, A consistent and accurate ab initio parametrization of density functional dispersion correction (DFT-D) for the 94 elements H-Pu., J. Chem. Phys. 132 (2010) 154104. https://doi.org/10.1063/1.3382344.

[6] S. Grimme, Density functional theory with London dispersion corrections, Wiley Interdiscip. Rev. Comput. Mol. Sci. 1 (2011) 211–228. https://doi.org/10.1002/wcms.30.

[7] E.R. Johnson, A.D. Becke, A post-Hartree–Fock model of intermolecular interactions, J. Chem. Phys. 123 (2005) 024101. https://doi.org/10.1063/1.1949201.

[8] S. Grimme, S. Ehrlich, L. Goerigk, Effect of the damping function in dispersion corrected density functional theory, J. Comput. Chem. 32 (2011) 1456–1465. https://doi.org/10.1002/jcc.21759.

[9] L. Versluis, T. Ziegler, The determination of molecular structures by density functional theory. The evaluation of analytical energy gradients by numerical integration, J. Chem. Phys. 88 (1988) 322–328. https://doi.org/10.1063/1.454603.

[10] C. Bannwarth, S. Ehlert, S. Grimme, GFN2-xTB—An Accurate and Broadly Parametrized Self-Consistent Tight-Binding Quantum Chemical Method with Multipole Electrostatics and Density-Dependent Dispersion Contributions, J. Chem. Theory Comput. 15 (2019) 1652–1671. https://doi.org/10.1021/acs.jctc.8b01176.

[11] C. Bannwarth, E. Caldeweyher, S. Ehlert, A. Hansen, P. Pracht, J. Seibert, S. Spicher, S. Grimme, Extended tight-binding quantum chemistry methods, WIREs Comput. Mol. Sci. 11 (2021) e1493. https://doi.org/10.1002/wcms.1493.

[12] A.G. Avent, D. Dubois, A. Pénicaud, R. Taylor, The minor isomers and IR spectrum of [84]fullerene, J. Chem. Soc. Perkin Trans. 2 (1997) 1907–1910. https://doi.org/10.1039/a703697c.

[13] M. Ernzerhof, G.E. Scuseria, Assessment of the Perdew–Burke–Ernzerhof exchange-correlation functional, J. Chem. Phys. 110 (1999) 5029. https://doi.org/10.1063/1.478401.

[14] T. Heine, C. Corminboeuf, G. Seifert, The magnetic shielding function of molecules and Pi-electron delocalization, Chem. Rev. 105 (2005) 3889–3910.

[15] G. Merino, T. Heine, G. Seifert, The Induced Magnetic Field in Cyclic Molecules, Chem. - A Eur. J. 10 (2004) 4367–4371. https://doi.org/10.1002/chem.200400457.

[16] R. Islas, T. Heine, G. Merino, The Induced Magnetic Field, Acc. Chem. Res. 45 (2012) 215–228. https://doi.org/10.1021/ar200117a.

Table S1. C_{60}-M distance (dC_{60}-M, Å), charge distribution (q^{C60} and q^{M}, |e|), and the Energy Decomposition Analysis (EDA) for the C_{60}-M interaction for the studied series (kcal/mol).

	dC_{60}-M	q^{C60}	q^{M}	ΔE_{Pauli}	ΔE_{elstat}	%[a]	ΔE_{orb}	%[a]	ΔE_{disp}	%[a]	ΔE_{int}
η^1-$[C_{60}Cu]^+$	1.942	0.60	0.40	84.4	-63.5	39.4	-94.7	58.7	-3.1	2.0	-76.9
η^2[6,6]-$[C_{60}Cu]^+$	2.052	0.62	0.38	80.5	-57.6	37.2	-94.1	60.8	-3.1	2.0	-74.3
η^2[5,6]-$[C_{60}Cu]^+$	2.042	0.61	0.39	86.0	-64.8	39.6	-95.6	58.5	-3.1	1.9	-77.5
η^1-$[C_{60}Ag]^+$	2.250	0.57	0.43	47.2	-35.7	35.2	-62.3	61.4	-3.4	3.3	-54.3
η^2[6,6]-$[C_{60}Ag]^+$	2.397	0.57	0.43	51.7	-36.3	35.2	-63.5	61.6	-3.4	3.3	-51.5
η^2[5,6]-$[C_{60}Ag]^+$	2.352	0.57	0.43	45.5	-34.8	35.2	-60.7	61.4	-3.4	3.4	-53.4
η^1-$[C_{60}Au]^+$	2.087	0.77	0.23	113.0	-83.9	40.2	-121.0	58.0	-3.9	1.9	-95.8
η^2[6,6]-$[C_{60}Au]^+$	2.229	0.74	0.26	112.4	-78.7	39.2	-118.3	58.9	-3.9	2.0	-88.6
η^2[5,6]-$[C_{60}Au]^+$	2.183	0.74	0.27	134.9	-98.3	43.0	-126.4	55.2	-4.1	1.8	-93.8

[a]Percentage denotes the relative contribution from stabilizing terms to the overall interaction energy.

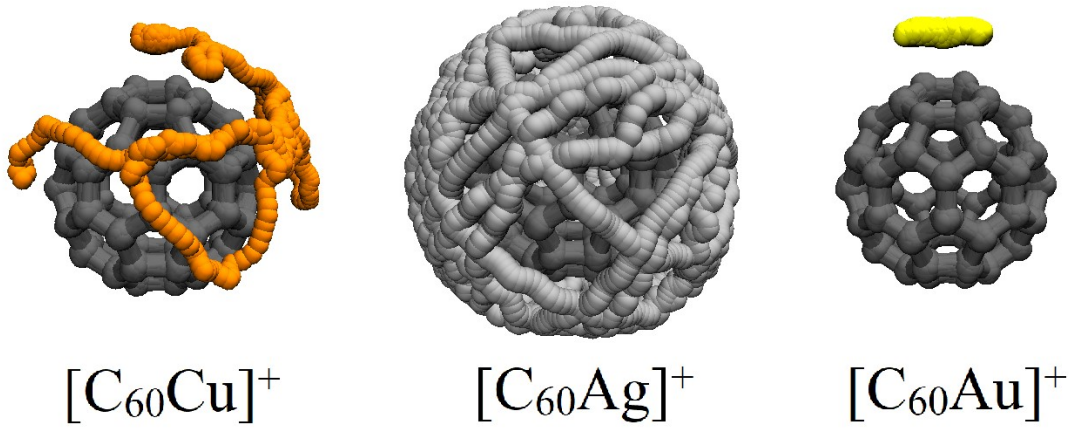

Figure S1. Molecular dynamics simulations (200 ps) revealing the distinct dynamic domains over the C_{60} fullerene surface at 400.15 K, denoting the overlap of all the metal trajectories.

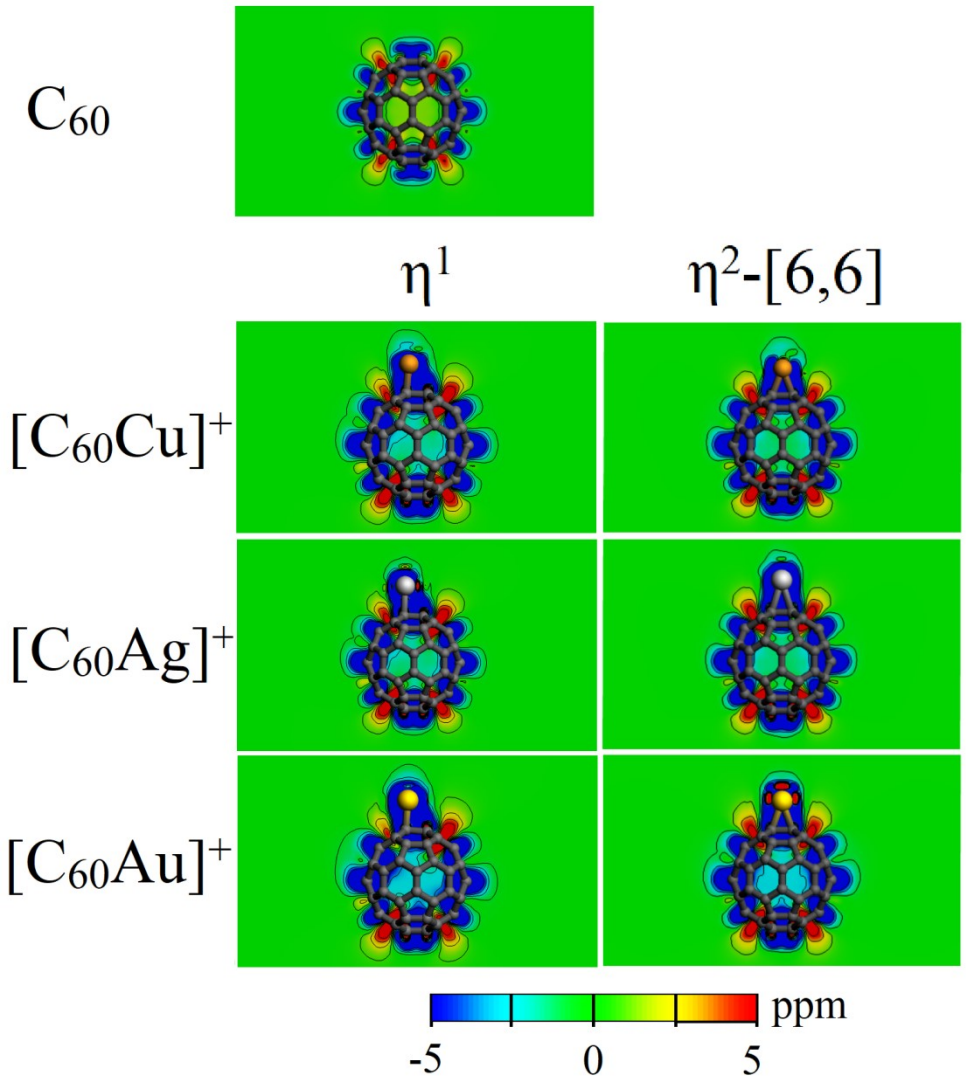

Figure S2. Contour plot representation of the magnetic response properties for the C_{60} and $[C_{60}M]^+$ species, accounting for NICS term. Negative values accounts for shielding regions, and positive values for deshielding regions.